



THEORETICAL INVESTIGATION OF WEAK INTERACTIONS BETWEEN DIATOMIC MOLECULES WITH DISTAL HISTIDINE ON THE HEME- MYOGLOBIN IN GAS AND SOLVENT MEDIUM

Mehrdad Khatami¹, Peyman Mohammadzadeh Jahani^{1*}, Maedeh Jafari², Alireza Khoshdel³, Hooshang Hamidian⁴

1. *Nanobioelectrochemistry Research Center, Bam University of Medical Sciences, Bam, Iran*
2. *Shiraz University of Medical Sciences, Shiraz, Iran*
3. *Clinical biochemistry department, Faculty of Medicine, Rafsanjan University of Medical Sciences, Rafsanjan, Iran*
4. *Department of Chemistry, Payame Noor University (PNU), Tehran, Iran*

ARTICLE INFO

Received:

03th May 2017

Received in revised form:

26th Sep 2017

Accepted:

28th Oct 2017

Available online:

14th Nov 2017

Keywords: *Heme- myoglobin, computational methods, solvent phase, hydrogen bond*

ABSTRACT

Hydrogen bond (HB) strength on the Heme- myoglobin models including O₂, CO and NO molecules binding to distal histidine (Heme-O₂, Heme-NO and Heme-CO) in gas and solvent mediums was studied by computational methods. Calculations in the solvent were well done using the self-consistent reaction field (SCRF) and discrete methods. Quantum theory of atoms in molecules (AIM) and natural bond orbital theory (NBO) were applied to obtain the topological data and charge transfer energies, respectively. Results of the calculations clearly showed that the solvent reduced the hydrogen bond energies compared to the gas phase. Furthermore, distal histidine of the Heme models in non-polar solvents formed the strongest hydrogen bond to the diatomic molecules with respect to polar solvents. All of the HB descriptor parameters such as structural, topological, NBO and vibrational frequencies parameters suggest that the Heme-O₂ has the strongest HB, which is followed by Heme-NO and Heme-CO, respectively. Totally, we obtained good correlations among Espinosa hydrogen bond energies with structural, topological, NBO and vibrational frequencies parameters in gas medium. Finally, based on the results we gained several linear equations in order to estimate of hydrogen bond energies in biological molecules.

Copyright © 2013 - All Rights Reserved - Pharmacophore

To Cite This Article: Mehrdad Khatami, Peyman Mohammadzadeh Jahani^{*}, Maedeh Jafari, Alireza Khoshdel, Hooshang Hamidian, (2017), "Theoretical Investigation of Weak Interactions between Diatomic Molecules with Distal Histidine on the Heme- Myoglobin in Gas and Solvent Medium", *Pharmacophore*, **8(6)**, 48-59.

Introduction

Myoglobin (Mb) is a conjugated protein which is the Oxygen molecule carrier in muscular tissues [1-3]. In Mb structure, there is a heme group for link to diatomic molecules such as O₂ and the so called Heme- myoglobin (Hmb) in this study. The bond between Hmb and O₂ is reversible which is both as O₂ storage and as a facilitator of the diffusion of O₂ from the capillaries to the mitochondria. In the heme structure, the iron atom is coordinated to a proximal histidine to make the iron five coordinated with a free site to bind O₂. Overhead the free site distal histidine is located with a weak interaction with the sixth iron ligand. The most important role of the distal histidine is assessment of diatomic molecules such as, NO and CO, favoring O₂ by mainly electrostatic interactions [4]. In the absence of distal histidine CO diatomic molecules in low concentration would prevent the Hmb and lead to suffocation. In vivo, Hmb finds substrate based on their shape and polarity. However, since the diatomic molecules O₂, NO and CO are similar in this respect, assessment of them is very difficult. The mechanism of recognition among these molecules in order to ease the favorable binding of O₂ to Hmb is especially important in the respiratory chain to avoid suffocation [5]. The high tendency of heme iron for link to NO and CO

makes them powerful inhibitors for Hmb and assessment between this species and O₂ molecule is of great importance for Hmb. The bond of O₂, NO and CO to heme iron has been studied both experimentally and theoretically [6–29]. Among the three studied diatomic species, the O₂ molecule form the weakest bond to iron with respect to others because the π^* -orbital of the O₂ molecule and the d_{z^2} -orbital on the iron have a favorable interaction [30].

The weak interaction of O₂, NO and CO to distal histidine on Hmb is represented by hydrogen bond (HB). Hydrogen bonds often have an affective role in molecular structures and they are a significant factor in many chemical and biochemical processes. However, they are almost stronger than Van der Waals interactions and dipole forces, but weaker than covalent and ionic bonds. The hydrogen bond usually exists in both inorganic and organic compounds for instance water, DNA and heme. This type of bond is very weak alone but when several hydrogen bonds form together between two molecules, the resulting union can be sufficiently strong as to be quite stable. Usually in biochemical systems the solvents are widely used. Whereas the solvent phase makes the changes in biological compounds weak interactions such as DNA hydrogen bonds and lead to mutation. Hence, the solvent will not be suitable in cell experiment. Besides in biological compounds two fundamental theoretical properties are their energy and structural parameters such as the type of bond, bond angles and torsional angles which are dependent on solvent effects. [31-36]

Since mentioned above the HB between diatomic molecules and distal histidine on Hmb is of great importance. In spite of this importance, suitable theoretical investigation for this type of weak interaction on the Hmb has not been reported. Hence we concluded that it is essential to perform a theoretical research about various aspects of this type of HB on the Hmb. The scope of this research is summarized as follows: (1) Investigation of the weak interactions such as HB on the Hmb by structural parameters, topological data, NBO analysis, vibration frequencies, (2) Calculation of the HB strength using Espinoza method on the Hmb, (3) Assessment of the effects of two different solvents on the nature of HB on Hmb by continuum and discretion models, (4) Survey of the linear relationship between the HB energies and HB descriptor parameters in gas phase on the Hmb, (5) Derivation of suitable linear equations in order to estimate the HB energies in the biological systems.

2. Computational Methods

In the present research we performed calculations by GAMESS software [37]. The output files were obtained at B3LYP/6-311++G (d,p) computational levels of theory. The atoms in molecules (AIM) and the natural bond orbital (NBO) programs were utilized to reach topological data and charge transfer energies, respectively. [38-41] Also, we used frequency calculations to assess the minima on the potential surface. To survey the solvent effects on the HB in the Heme models we applied, two different solvent phases, one water ($\epsilon = 80.1$) and the other carbon tetrachloride ($\epsilon = 2.24$). In this case, we employed the self-consistent reaction field (SCRF) method including the polarized continuum models (PCM, IPCM, SCIPCM) [46-53]. Furthermore, the solvent effect in discrete model for individual solute-solvent interactions was performed by a set of either one or two solvent molecules around the active sites of the Heme models. Finally, the HB energies were estimated by Espinoza method [42-44].

3. Theoretical section

3.1. Effects of the structural parameters on HB

In this article, we showed the Heme as an individual molecule including the proximal histidine in Fig.1. Also, the formed HB between O₂, CO, NO and the distal histidine on the Hmb is shown in Fig.2. The models are represented by Heme-O₂, Heme-NO and Heme-CO. Optimization calculations on the models to obtain the real structures and HB energies in the gas phase and solvents mediums were performed at B3LYP/6-311++G (d,p) computational levels of theory. In the continuum solvent methods we used $\epsilon = 78.39$ and $\epsilon = 2.24$ in order to simulate the water and carbon tetrachloride solutions, respectively. Also, in the discretion methods, either one or two water and carbon tetrachloride molecules were chosen near the active site of the Heme models in the optimized gas phase structures, and optimization calculations were performed on them. The optimized structures of the models including water molecules are presented in Fig.3. The calculated structural parameters of the models in different solvents and gas phase are displayed in Table 1.

The distal histidine in the Heme models link to diatomic molecules by N-H...O-X-Heme (X=C, N, O) hydrogen bond. In these cases, N atom (from histidine) plays the role of the proton donor and O atom (from diatomic molecules) is the proton acceptor. The structural parameters such as $R_{O...H}$, R_{N-H} and θ_{NHO} are usually used to estimate the HB strength. The large values of R_{N-H} , θ_{NHO} and the small values of the $R_{O...H}$ are accompanied by the larger values of HB energies. According to the calculated structural parameters shown in Table.1, the values of $R_{O...H}$, R_{N-H} and θ_{NHO} for Heme-O₂ and Heme-CO models are about 0.996, 0.945, 1.87 and 2.11Å, respectively. These values clearly show the strongest and the weakest HB interaction in these models. Also, the values of θ_{NHO} for these models are about 144.7° and 135.9° which are in consisting of the previous result. The structural parameters of the Heme models change in the solvent mediums. The results of the solvent effect are shown in table .1, revealing that the solvent slightly reduced the HB strength. Also, when water is used as a polar solvent, the HB strength is more reduced with respect to carbon tetrachloride in the role of the non-polar solvent. Theoretical calculations show that the $R_{O...H}$ increase while the R_{N-H} and θ_{NHO} decrease when water is used as a polar solvent medium in all of the Heme models. The results of Table.1 clearly show that the least value of $R_{O...H}$ and the most value of R_{N-H} and

θ_{NH_2} belong to Heme-O₂, reflecting the strongest O...H interaction in both of the solvents. For example, the $R_{\text{O}\dots\text{H}}$ and $R_{\text{N}\dots\text{H}}$ and θ_{NH_2} for the N-H...O bridge in Heme-O₂(the strongest model) and Heme-CO(the weakest model) change to 1.89 Å, 2.14 Å, 0.990 Å, 0.933 Å, 140.9° and 134.5° in water solution, respectively. Our results in other systems such as PCM, IPCM and SCIPCM are also in good agreement with these conclusions (see Table 1).

3.2. Topological data on HB

Topological data extracted from AIM software were used to estimate the HB strength. The calculated topological parameters including electron density (ρ), Laplacian electron density ($\nabla^2\rho$), density of the total energy of electrons (H), kinetic (G) and potential (V) electron energy densities of the Heme models are presented in Table 2. Based on the results of Table.2, the minimum and maximum values of ρ_{BCP} and $\nabla^2\rho_{\text{BCP}}$ in the gas, water and carbon tetrachloride for O...H bonding at the Heme models were 0.0267–0.0321, 0.1023-0.1156, 0.0260- 0.0317, 0.1016-0.1123, 0.0263–0.0319 and 0.1020-0.1125, respectively. The $\nabla^2\rho_{\text{BCP}}$ positive values showed that O...H interactions were electrostatic. The largest ρ_{BCP} value was for Heme-O₂ with the minimum of O...H bond length (see Table.1). The results of AIM analysis showed that greater ρ_{BCP} at O...H bond length was related to the greater strength of HB in the Heme models. Also, the minimum value of ρ_{BCP} O...H was observed for Heme-CO that is in agreement with the weakest HB in Heme models. Also, in this article we found a good correlation between topological and structural parameters for the investigated Heme models. The linear relationship between O...H bond length- electron density and O...H bond Length-Laplacian electron density are shown in the following equations with a correlation coefficient of 0. 0.992 and 0.929, respectively. (See Fig.4):

$$R_{\text{O}\dots\text{H}} = -102.56 \rho_{\text{O}\dots\text{H}} + 5.1531 \quad R=0.992$$

$$R_{\text{O}\dots\text{H}} = -18.55 \nabla^2\rho_{\text{O}\dots\text{H}} + 3.991 \quad R=0.929$$

Hence, based on these equations the topological properties can be used for evaluation of the structural parameters in Heme models and similar biological systems. Furthermore, AIM analysis results in the solvent mediums illustrated that ρ_{BCP} and $\nabla^2\rho_{\text{BCP}}$ values decreased especially when water was simulated as the polar solvent (see Table.2). Finally, the density of total energy calculations including kinetic (G) and potential (V) electron energy densities in the solvent and gas medium showed that the values of G were positive and the values of V were negative. These results showed that HB interaction between diatomic molecules and distal histidine in the Heme models had the covalent nature.

3.3. NBO analysis on HB

In this research, we used NBO analysis data for the confirmation of the HB strength order in the Heme models at the different mediums. Usually in NBO analysis, the most important descriptor parameter of HB is charge transfer from the lone pairs of proton acceptor to the proton donor antibond orbital. It's well known that the occupation numbers and their energies of orbitals change due to this charge transfer. As mentioned above, in the studied models the lone pairs of O atom $lp_{(\text{O})}$ from Heme are used as the donor and $\sigma^*_{\text{N}\dots\text{H}}$ antibonds from distal histidine are as the acceptor. The interaction energies ($lp_{(\text{O})} \rightarrow \sigma^*_{\text{N}\dots\text{H}}$), the NBO occupation numbers (n), their respective orbital energies (ϵ), occupation numbers difference (Δn)(Hydrogen bonded form-Non hydrogen bonded form) and orbital energies difference ($\Delta\epsilon$) in the different mediums were evaluated and gathered in Tables 3 and 4. According to the data in these Tables, there was a considerable difference between the NBO parameters of the Heme models. For instance, The Calculated interaction energies ($lp_{(\text{O})} \rightarrow \sigma^*_{\text{N}\dots\text{H}}$), difference occupation numbers (Δn)($lp_{(\text{O})}, \sigma^*_{\text{N}\dots\text{H}}$) and difference orbital energies ($\Delta\epsilon$)($lp_{(\text{O})}, \sigma^*_{\text{N}\dots\text{H}}$) in the gas phase for (Heme-O₂, Heme-CO and Heme-NO) were about (15.43, 7.953 and 9.321 kcal mol⁻¹), (0.021, 0.017, 0.005, 0.007, 0.014 and 0.013) and (0.0051, 0.039, 0.0019, 0.014, 0.0037 and 0.028 kcal mol⁻¹), respectively.

These data clearly show that there are more interaction energies ($lp_{(\text{O})} \rightarrow \sigma^*_{\text{N}\dots\text{H}}$), difference occupation number and energy in Heme-O₂ with respect to others. This means that the HB in Heme-O₂ is stronger which is follows with the Heme-NO and Heme-CO. Furthermore, inspection on the data in the water medium (polar solvent) in discrete and continuum methods for all of the investigated Heme models showed that the values of the $lp_{(\text{O})}$, $\sigma^*_{\text{N}\dots\text{H}}$, Δn and $\Delta\epsilon$ considerably decreased, this proves the weaker HB in these models in comparison with carbon tetrachloride(non-polar solvent) and gas medium. In this section, it seems that it is necessary to study the correlations between some of the NBO parameters with the structural and topological parameters. The $E^{(2)}_{lp_{(\text{O})} \rightarrow \sigma^*_{\text{N}\dots\text{H}}} - R_{\text{O}\dots\text{H}}$, $E^{(2)}_{lp_{(\text{O})} \rightarrow \sigma^*_{\text{N}\dots\text{H}}} - \rho_{\text{BCP}}$, $E^{(2)}_{lp_{(\text{O})} \rightarrow \sigma^*_{\text{N}\dots\text{H}}} - R_{\text{N}\dots\text{H}}$, $\Delta n(lp \text{ and } \sigma^*) - \rho_{\text{BCP}}$ and $\Delta\epsilon(lp \text{ and } \sigma^*) - \rho_{\text{BCP}}$ linear relationship for the Heme models in gas were found with correlation coefficients of 0.968, 0.982, 0.991, 0.957, 0.973, 0.965 and 0.956 respectively. The excellent correlation between NBO parameters with the structural and topological parameters are shown as below:

$$R_{\text{O}\dots\text{H}} = 0.033 E^{(2)}_{lp_{(\text{O})} \rightarrow \sigma^*_{\text{N}\dots\text{H}}} + 2.366 R = 0.968$$

$$R_{\text{N}\dots\text{H}} = 0.007 E^{(2)}_{lp_{(\text{O})} \rightarrow \sigma^*_{\text{N}\dots\text{H}}} + 0.891 R = 0.982$$

$$\rho_{\text{O}\dots\text{H}} = 0.0003 E^{(2)}_{lp_{(\text{O})} \rightarrow \sigma^*_{\text{N}\dots\text{H}}} + 0.027 R = 0.991$$

$$\rho_{\text{O}\dots\text{H}} = 0.152 \Delta n lp + 0.0291 R = 0.957$$

$$\rho_{\text{O}\dots\text{H}} = 0.244 \Delta n \sigma^* + 0.0281 R = 0.973$$

$$\rho_{\text{O}\dots\text{H}} = 0.788 \Delta\epsilon lp + 0.0283 R = 0.965$$

$$\rho_{\text{O}\dots\text{H}} = 0.097 \Delta\epsilon \sigma^* + 0.0285 R = 0.956$$

3.4. Vibration frequencies analysis on the HB

The vibration frequencies are appropriate parameters in evaluation of HB. In order to confirm the results of the previous sections, we performed vibration frequencies analysis. In this analysis, stretching vibration frequencies changes of the N-H bond between the non-hydrogen bonded forms (distal histidine) and hydrogen bonded forms (Heme myoglobin) were the most important parameter for estimation of the HB strength. Basically, HB formation decreases the vibration frequencies of the N-H bond from the distal histidine which is involved in HB. The calculated stretching vibrational frequencies $V(N-H)_{his}$ in the non-hydrogen bonded forms, $V(N-H)_{myo}$ in the hydrogen bonded forms and stretching vibrational frequencies difference $\Delta v(N-H) (V(N-H)_{myo} - V(N-H)_{his})$ in different mediums of the Heme models are listed in Table 5. As shown in Table 5, there was a significant difference between the $\Delta v(N-H)$ of Heme models. For instance, The Calculated $\Delta v(N-H)$ in the gas phase for Heme-O₂, Heme-CO and Heme-NO were about 85.759, 61.762 and 79.604 kcalmol⁻¹, respectively.

These results indicated that the maximum $\Delta v(N-H)$ observed for Heme-O₂ was associated with the maximum N-H bond length (in gas, $R_{N-H} = 0.996 \text{ \AA}$). The results of the calculated vibrational frequencies indicated that the lengthening distance and greater vibrational frequencies difference ($\Delta v(N-H)$) at N-H bond confirm the greater strength of HB in the Heme models. Besides, in the Heme-CO with the weakest HB strength among Heme models there was the smallest value of $\Delta v(N-H)$. Also, when water was used as the polar solvent $\Delta v(N-H)$ greatly decreased which was followed by non-polar solvent and gas phase in Heme models. Finally, in order to obtain dependency among the structural, topological, NBO and vibrational frequencies parameters, we investigated the correlations between N-H, O...H bond lengths, O...H electron density and interaction energy $E^{(2)}_{lp(O)_- \sigma^*N-H}$ versus $\Delta v(N-H)$, the $\Delta v(N-H) - R_{N-H}$, $\Delta v(N-H) - R_{O...H}$, $\Delta v(N-H) - \rho_{O...H}$ and $\Delta v(N-H) - E^{(2)}_{lp(O)_- \sigma^*N-H}$ linear relationship for the Heme models in gas phase are found with a correlation coefficients of 0.9534, 0.9913, 1 and 0.992 respectively. Due to appropriate linear correlations among these parameters some of the following equations were obtained.

$$\Delta v(N-H) = 96.51 R_{O...H} + 265.2 R = 0.9913$$

$$\Delta v(N-H) = 476.4 R_{N-H} + 387.1 R = 0.9534$$

$$\Delta v(N-H) = 9978.8 \rho_{O...H} + 234.63 R = 1$$

$$\Delta v(N-H) = 3.263 E^{(2)}_{lp(O)_- \sigma^*N-H} + 36.22 R = 0.992$$

3.5. Hydrogen bond energies and its linear relationship with descriptor HB parameters

In this study, we used the Espinosa method to calculate the HB energies [42, 44]. In Espinosa, half of the potential energy density of O...H bond at the critical point is considered as HB energy. The calculated HB energies in different mediums for Heme models are shown in Table.5. From Espinosa method data in this Table, the HB energy (E_{HB}) of Heme-O₂, Heme-NO and Heme-CO in gas are 39.5, 39.1 and 36.8 kcalmol⁻¹, respectively. These results are in agreement with the structural, topological, NBO and vibrational frequencies conclusions. Furthermore, the calculated HB energies in the two solvents (water and carbon tetrachloride in discrete and continuum models) for all of the Heme models showed that HB energies in the polar solvents reduced followed by non-polar solvents and gas phase (see Table.5). This result is also in line with the previous conclusions. In addition, in order to obtain a series of linear equations for estimation of the HB strength in the biological systems, the correlations between E_{HB} and some of the descriptor HB parameters such as structural, topological, NBO and vibrational frequencies parameters were studied. First we explored the relationship between E_{HB} and structural parameters. The $E_{HB} - R_{O...H}$, $E_{HB} - R_{N-H}$ and $E_{HB} - \theta_{NHO}$ linear relationship for the Heme models in gas phase were found with correlation coefficients of 0.999, 0.895 and 0.964, respectively. Due to this acceptable correlation (except of R_{N-H}), we extracted some of the appropriate equations to estimate the HB energies versus the structural parameters in biological systems. These equations are as below:

$$E_{HB} = -11.33 R_{O...H} + 60.71 R = 0.999$$

$$E_{HB} = 53.98 R_{N-H} + 13.97 R = 0.895$$

$$E_{HB} = 0.319 \theta_{NHO} + 6.448 R = 0.964$$

Also, the topological parameters can be used in calculation of the HB energies in most of the biochemical systems [45, 46]. The comparable diagrams for correlations between E_{HB} and topological parameters are shown in Figure 4. It is obvious from the diagrams that correlation between E_{HB} and the topological parameters are acceptable and equations are shown as below:

$$E_{HB} = 1160.3 \rho_{O...H} + 2.382 R = 0.989$$

$$E_{HB} = 209.2 V^2 \rho + 15.60 R = 0.920$$

$$E_{HB} = -12.82 V_{BCP} + 0.876 R = 1$$

The results of Espinosa and Molins's study [45,46] support these conclusions in predication of HB energies in biochemical compounds. The natural bond orbital (NBO) parameters have been used to evaluate the HB energies [47]. The HB Espinosa energy (E_{HB}) has an appropriate correlation with interaction energy $E^{(2)}_{lp(O)_- \sigma^*N-H}$ for Heme models in gas phase that is shown as below:

$$E_{HB} = 0.375 E^{(2)}_{lp(O)_- \sigma^*N-H} + 33.92 R = 0.961$$

Finally, based on the a good relation between E_{HB} and stretching vibrational frequencies difference $\Delta\nu(N-H)$ for Heme models in gas phase, we can conclude that E_{HB} will easily be evaluated from vibrational frequencies analysis. The corresponding equation is as below:

$$E_{HB} = 0.1162 \Delta\nu(N-H) + 29.67R = 0.988$$

4. Conclusions

In this article, the weak HB interactions between the diatomic molecules as O_2 , CO and NO with the distal histidine in the Heme myoglobin were investigated by DFT calculations. Also, in order to reach the real simulation of the Heme myoglobin in vivo, the calculations were performed in water and carbon tetrachloride as polar and non-polar solvents, respectively. The structural parameters results showed that the large values of R_{N-H} , θ_{NHO} and the small values of the $R_{O...H}$ were accompanied by the larger values of HB energies in the gas and solution mediums for all of the Heme models. The atoms in molecule theory (AIM) were used and its results indicated that the shorter distance and greater ρ and $\nabla^2 \rho$ at $O...H$ bond length was related to the greater strength of HB in the Heme models for all of the mediums. Also, the natural bond orbital analysis showed that higher interaction energies $E^{(2)}_{lp(O)... \sigma^*_{N-H}}$ and more difference occupation numbers and energies, reflect the strongest $O...H$ interaction in Heme models in all of the mediums. The calculated vibrational frequencies are in line with the structural, topological and NBO data and suggest that the lengthening distance and greater vibrational frequencies difference ($\Delta\nu(N-H)$) at $N-H$ bond length can be related to the greater strength of HB in the Heme models. Totally, the results of the solvent effect revealed that the solvent slightly reduced the HB strength. Also, when water was the polar solvent used the HB strength is more reduced with respect to carbon tetrachloride in the role of the non-polar solvent.

All of the descriptor HB parameters such as structural, topological, NBO and vibrational frequencies confirm that the Heme- O_2 has the strongest HB, followed by Heme-NO and Heme-CO. Furthermore, in this study we found an appropriate relationship between structural, topological, NBO and vibrational frequencies parameters for all of the studied models. Espinosa method was used to estimate the HB energies in the Heme models and its results are in the same line with those of the descriptor HB parameters. Finally, the correlations between E_{HB} and the descriptor HB parameters for Heme models were investigated. The results showed that E_{HB} strongly correlated with $O...H$ and $N-H$ bonds. Furthermore, there was an acceptable relationship between E_{HB} and AIM data such as ρ and $\nabla^2 \rho$ and $V(r)$ at HB critical point. Also E_{HB} well correlated with interaction energies $E^{(2)}_{lp(O)... \sigma^*_{N-H}}$ and vibrational frequencies difference ($\Delta\nu(N-H)$). The obtained linear equations between E_{HB} and the descriptor HB parameters revealed that the Espinosa was an appropriate method of evaluation of the HB energies in these systems and these equations could be applied for measurement of the HB energies in Heme models and other biochemical compounds.

Acknowledgement:

We gratefully thank Bam University of Medical Sciences for financial support.

Funding Information

This study was not funded by university or organizations.

Compliance with ethical standards

Conflict of interest

The authors declare that they have no conflict of interest.

Ethical approval

This article does not contain any studies with human participants or animals performed by any of the authors

Reference

1. Berg J M, Tymoczko J L, Stryer L (2002). Biochemistry 5th ed W H Freeman New York
2. Parak F G, Nienhaus G U (2002) Chem Phys Chem 3: 249–254
3. Perutz M F (1990) Trends Biochem Sci 14: 42–44
4. Olson J S, Phillips Jr G N (1997) J Biol Inorg Chem 2: 544– 552
5. Mattias Blomberg L, Margareta R A, Blomberg, Siegbahn P E M (2005) J Inorg Biochem 99: 949–958
6. Jocley Queiroz Araujo, a Jose´ Walkimar de Mesquita Carneiro a b, Martha Teixeira de Araujo, c Franco Henrique Andrade Leited, e and Alex Gutterres Tarantod (2008) BIOORGAN MED CHEM 16: 5021–5029
7. Alberto De Petris a, Maria Elisa Crestoni a, Adele Piroli b, Carme Rovira c d, Javier Iglesias-Fernández c, Barbara Chiavarino a, Rino Ragnò b, Simonetta Fornarini(2015) Polyhedron 90: 245–251
8. Yuqi Li, Savita K, Sharma Kenneth D Karlin (2013) Polyhedron 58: 190–196
9. Kaustuv Mitra, Kushal Sengupta, Asmita Singha, Sabyasachi Bandyopadhyay, Sudipta Chatterjee, Atanu Rana, Subhra Samanta, Abhishek (2016) J. Inorg. Biochem 155: 82–91
10. Mary Grace I, Galinato a, Robert S, Fogle III a, Amanda Stetz a, Jenny F Galan (2016) J Inorg Biochem 154: 7–20
11. Lauren E, Goodrich, Nicolai Lehnert (2013) J Inorg Biochem 118: 179–186

12. Blomberg L M, Blomberg M R A, Siegbahn P E M (2004) *J Biol Inorg Chem* 9: 923–935
13. Yasunori Y, Hiroyuki S, Masaki M (2007) *J Inorg Biochem* 101: 1410–1427
14. Pietro Vidossich a, Mercedes Alfonso-Prieto b, Carme R (2012) *Journal J Inorg Biochem* 117: 292–297
15. Frisch M J et al (2003) *Gaussian 03 Revision B 03* Gaussian Inc Pittsburgh PA
16. Schrödinger (2000) Inc Portland Oregon Jaguar 4: 2
17. Jing D, Masanori S, John H D (2011) *Coord. Chem. Rev* 255: 700–716
18. Tigran S, Kurtikyan a b, Peter C F (2008) *Coord. Chem. Rev* 252: 1486–1496
19. Ivan D, Risto M N, Carme R (2006) *Biophys J* 91: 2024–2034
20. Curtiis L A, Raghavachari K, Redfern R C, Pople J A (2000) *J Chem Phys* 112: 7374–7383
21. Siegbahn P E M, Blomberg M RA (2000) *Chem Rev* 100: 421– 437
22. Blomberg M RA, Siegbahn P E M (2001) *J Phys Chem B* 105: 9375–9386
23. Sigfridsson E, Ryde U J (2002) *Inorg. Biochem* 91: 101–115
24. Jensen K P, Roos B O, Ryde U J (2005) *Inorg Biochem* 99: 45–54
25. Harvey J N (2000) *J Am Chem Soc* 122: 12401–12402
26. Harvey J N (2004) *Faraday Discuss* 127: 165–177
27. Franzen S (2002) *Proc Natl Acad Sci USA* 99: 16754–16759
28. Harvey J N (2000) *J Am Chem Soc* 122:12401–12402
29. Harvey J N (2004) *Faraday Discuss* 127:165–177
30. Hoffmann R, Chen M M-L, Thorn D L (1977) *Inorg Chem* 16: 503–511
31. Zhao G J, Han K L (2012) *Acc Chem Res* 45: 404–413
32. Zhao G, Yu F, Zhang M, Northrop B, Yang H, Han K, Stang P (2011) *J Phys Chem A* 115: 6390–6393
33. CAO X, LIU C, LIU Y (2012) *Theor Comput Chem* 11: 573–586
34. Glasbeek M, Zhang H (2004) *Chem Rev* 104: 1929–1954
35. Shahabi M, Raissi H, Mollania F (2015) *Struct Chem* 26: 491–506
36. Mollania F, Raissi H (2014) *Struct Chem* 25: 1099–1109
37. Gordon M S, Schmidt M W, Dykstra C E, Frenking G, Kim K S, Scuseria G E (2005) *Theory and Applications of Computational Chemistry: the first forty years and Advances in electronic structure theory: GAMESS a decade later*, 1167–1189.
38. Bader R F W, (1990) *Atoms in Molecules—A Quantum Theory*, Clarendon Press Oxford
39. AIM2000 designed by Friedrich Biegler-König, University of Applied Sciences, Bielefeld, 2000
40. Biegler-König F W, Bader R FW, Tang Y H, Tal Y (1982) *J Comput Chem* 3: 317–328
41. Glendening E D, Badenhoop J K, Reed A E, Carpenter J E, Bohmann J A, Morales C M, Weinhold F (2001) *Theoretical Chemistry Institute University of Wisconsin Madison WI*
42. Espinosa E, Molins E (2000) *J Chem Phys* 113:5686–5694
43. Espinosa E, Souhassou M, Lachekar H, Lecomte(1999) *C Acta Crystallogr B* 55: 563–572
44. Abramov Y A (1997) *Acta Crystallogr A* 53: 264–272
45. Grabowski S J (2000) *J Phys Chem* 104A: 5551
46. Espinosa E, Molins E (2000) *J Chem Phys* 113: 5686
47. Alabugin I V, Manoharam M, Feabody S, Weinhold F (2003) *J Am Chem Soc* 125: 5973

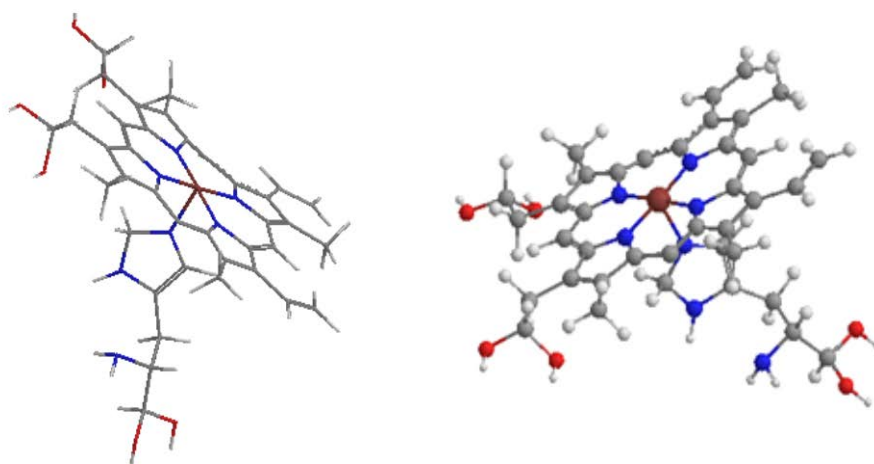


Fig. 1. The structure of myoglobin including the proximal histidine.

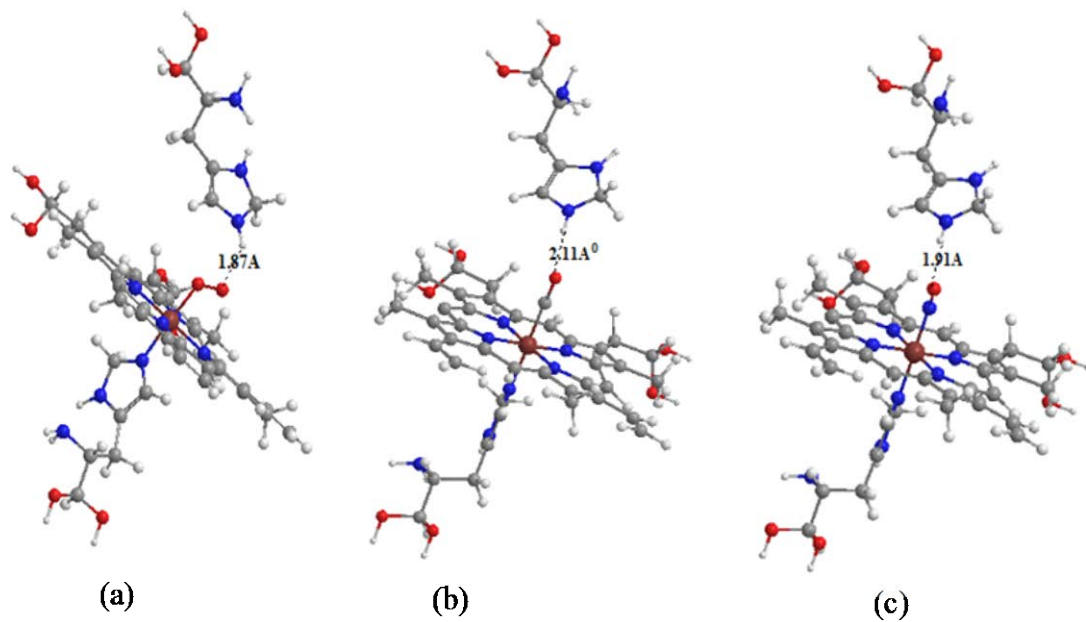


Fig.2. (a) The binding of molecular oxygen, (b) carbon monoxide and (c) nitric oxide to the heme -myoglobin.

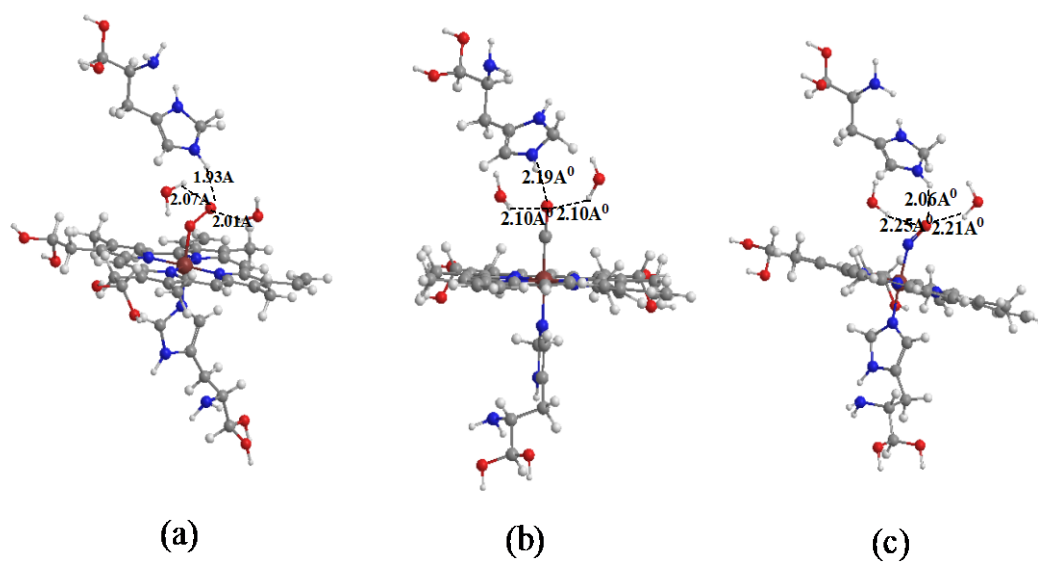


Fig.3. (a) The binding of molecular oxygen, (b) carbon monoxide and (c) nitric oxide to the heme -myoglobin including water molecules.

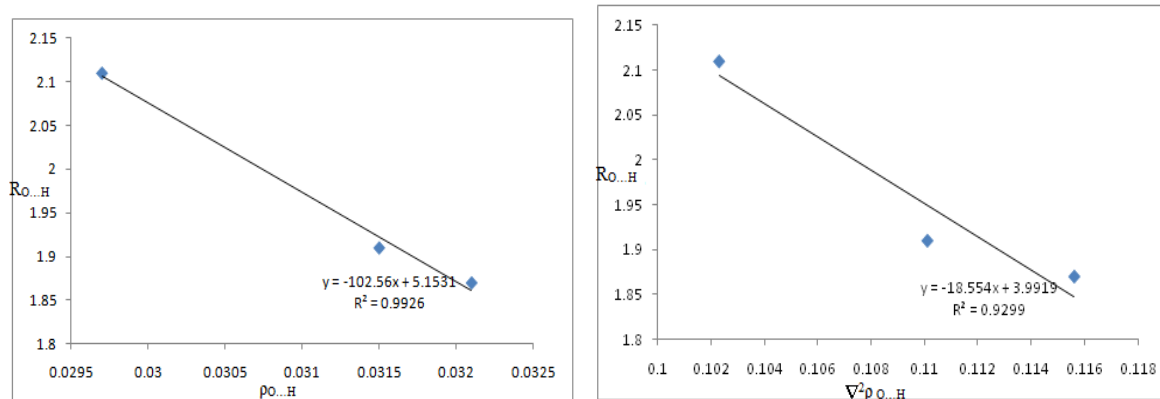


Fig. 4. The relationship between the $R_{(O...H)}$ versus $\rho_{O...H}$ and $\nabla^2\rho_{O...H}$.

Table 1. The calculated geometrical parameters (A^0) of the Heme models in solvents and gas phase.

Geometrical parameters	$R_{(O...H)}$	$R_{(Fe...X_2)}$	$R_{(N-H)}$	θ_{NHO}
Gas phase				
Heme-O ₂	1.87	1.88	0.996	144.7
Heme-CO	2.11	1.78	0.945	135.9
Heme-NO	1.91	1.81	0.973	141.8
1H ₂ O(CCl ₄)				
Heme-O ₂	1.89(1.88)	-	0.990(0.992)	140.9(142.6)
Heme-CO	2.14(2.12)	-	0.933(0.939)	134.5(134.9)
Heme-NO	1.97(1.93)	-	0.971(0.972)	138.2(138.9)
2H ₂ O(2CCl ₄)				
Heme-O ₂	1.93(1.90)	-	0.950(0.975)	139.0(141.1)
Heme-CO	2.19(2.15)	-	0.899(0.907)	133.2(134.2)
Heme-NO	2.06(2.01)	-	0.922(0.955)	137.8(138.2)
PCM				
Heme-O ₂	1.92(1.90)	-	0.946(0.951)	135.8(140.9)
Heme-CO	2.21(2.13)	-	0.887(0.903)	131.7(133.9)
Heme-NO	2.05(2.02)	-	0.924(0.938)	134.0(135.4)
IPCM				
Heme-O ₂	1.92(1.91)	-	0.947(0.954)	136.0(141.3)
Heme-CO	2.22(2.17)	-	0.889(0.905)	132.4(134.0)
Heme-NO	2.05(2.02)	-	0.925(0.941)	134.3(135.6)
SCIPCM				
Heme-O ₂	1.92(1.91)	-	0.948(0.953)	136.0(141.2)
Heme-CO	2.23(2.19)	-	0.890(0.906)	132.7(133.9)
Heme-NO	2.07(2.03)	-	0.927(0.939)	135.7(136.3)

Values in parentheses refer to calculation in the carbon tetra chloride solution.

Table 2. The selected topological parameters of investigated Heme models and the density of the total energy of electrons (H) and its two components, the kinetic (G) and potential (V) electron energy densities (in a.u.) in solvents and gas phase

Topological parameters	$\rho_{BCP(O...H)}$	$\nabla^2\rho_{BCP(O...H)}$	$V_{BCP(O...H)}$	$G_{BCP(O...H)}$	$H_{BCP(O...H)}$
Gas phase					
Heme-O ₂	0.0321	0.1156	-0.0301	0.0296	-0.0005
Heme-CO	0.0297	0.1023	-0.0280	0.0270	-0.0010
Heme-NO	0.0315	0.1101	-0.0298	0.0284	-0.0014
1H ₂ O(CCl ₄)					
Heme-O ₂	0.0317 (0.0319)	0.1123 (0.1125)	-0.0283 (-0.0289)	0.0276 (0.0286)	-0.0007 (-0.0003)

Heme-CO	0.0260 (0.0263)	0.1016 (0.1020)	-0.0261 (-0.0271)	0.0245 (0.0265)	-0.0016 (-0.0006)
Heme-NO	0.0298 (0.0300)	0.1087 (0.1094)	-0.0275 (-0.0279)	0.0263 (0.0277)	0.0012 (-0.0002)
2H ₂ O(CCl ₄)					
Heme-O ₂	0.0305 (0.0311)	0.1108 (0.1127)	-0.0264 (-0.0279)	0.0256 (0.0276)	-0.0008 (-0.0003)
Heme-CO	0.0242 (0.0259)	0.1002 (0.1016)	-0.0223 (-0.0225)	0.0214 (0.0231)	-0.0009 (-0.0006)
Heme-NO	0.0263 (0.0282)	0.1065 (0.1089)	-0.0251 (-0.0261)	0.0244 (0.0258)	-0.0007 (-0.0003)
PCM					
Heme-O ₂	0.0307 (0.0314)	0.1112 (0.1130)	-0.0257 (-0.0282)	0.0255 (0.0279)	-0.0002 (-0.0003)
Heme-CO	0.0240 (0.0261)	0.1010 (0.1012)	-0.0219 (-0.0229)	0.0217 (0.0223)	-0.0002 (-0.0006)
Heme-NO	0.0266 (0.0288)	0.1064 (0.1092)	-0.0243 (-0.0267)	0.0235 (0.0251)	-0.0008 (-0.0016)
IPCM					
Heme-O ₂	0.0307 (0.0313)	0.1111 (0.1131)	-0.0261 (-0.0281)	0.0258 (0.0277)	-0.0003 (-0.0004)
Heme-CO	0.0244 (0.0265)	0.1013 (0.1018)	-0.0219 (-0.0233)	0.0218 (0.0224)	-0.0001 (-0.0009)
Heme-NO	0.0268 (0.0291)	0.1066 (0.1097)	-0.0238 (-0.0265)	0.0235 (0.0247)	-0.0003 (-0.0018)
SCIPCM					
Heme-O ₂	0.0309 (0.0312)	0.1114 (0.1133)	-0.0259 (-0.0285)	0.0257 (0.0272)	-0.0002 (-0.0013)
Heme-CO	0.0242 (0.0260)	0.1013 (0.1015)	-0.0220 (-0.0226)	0.0219 (0.0231)	-0.0001 (-0.0005)
Heme-NO	0.0264 (0.0289)	0.1067 (0.1094)	-0.0240 (-0.0261)	0.0231 (0.0245)	-0.0009 (-0.016)

Values in parentheses refer to calculation in carbon tetra chloride solution.

Table 3. The occupation number labeled as ON with corresponding energies presented and the selected charge transfer energies of the Heme models in water and gas phase (kcal mol⁻¹)

NBO parameters	$E_{LP-\sigma^*N-H}^2$	$ON_{(LP)}/\Delta n_{LP}$	$ON_{\sigma^*NH}/\Delta n_{\sigma^*NH}$	$E_{LP}/\Delta E_{LP}$	$E_{\sigma^*NH}/\Delta E_{\sigma^*NH}$
Gas phase					
Heme-O ₂	15.43	1.922(1.901) /0.021	0.01663 (0.03363) /0.017	-0.3861(-0.3811) /0.0051	0.39355 (0.35457) /0.039
Heme-CO	7.953	1.899(1.894) /0.005	0.01663 (0.02374) /0.007	-0.2987(-0.2968) /0.0019	0.39355 (0.37948) /0.014
Heme-NO	12.92	1.911(1.897) /0.014	0.01663 (0.02992) /0.013	-0.3211(-0.3174) /0.0037	0.39355 (0.36549) /0.028
1H ₂ O					

Heme-O ₂	12.80	1.894(1.886) /0.008	0.01663 (0.01890)/ /0.0023	-0.3711(-0.3667) /0.0044	0.39355 (0.37653)/ /0.017
Heme-CO	6.632	1.861(1.859)/ /0.002	0.01663 (0.01699)/ /0.0003	-0.2890(-0.2879) /0.0011	0.39355 (0.39173)/ /0.0018
Heme-NO	11.51	1.871(1.867)/ /0.004	0.01663 (0.01761) /0.0010	-0.3152(-0.3127) /0.0025	0.39355 (0.39061)/ /0.0029
2H ₂ O					
Heme-O ₂	12.10	1.804(1.798)/ /0.006	0.01663 (0.01845) /0.0018	-0.3265(-0.3238) /0.0027	0.39355 (0.39095)/ /0.0026
Heme-CO	6.341	1.762(1.759)/ /0.003	0.01663 (0.01711)/ /0.0005	-0.2765(-0.2760) /0.0005	0.39355 (0.39311)/ /0.0004
Heme-NO	9.931	1.772(1.768)/ /0.004	0.01663 (0.01739)/ /0.0007	-0.3089(-0.3080) /0.0009	0.39355 (0.39294)/ /0.0006
PCM					
Heme-O ₂	11.23	1.799(1.790)/ /0.009	0.01983(0.02170) /0.0019	-0.3271(-0.3245) /0.0026	0.34761(0.34456)/ /0.0031
Heme-CO	7.292	1.758(1.754)/ /0.004	0.01983 (0.02059)/ /0.0007	-0.2754(-0.2748) /0.0006	0.34761 (0.347014)/ /0.0006
Heme-NO	8.579	1.774(1.768)/ /0.006	0.01983 (0.02082)/ /0.0010	-0.3093(-0.3082) /0.0011	0.34761 (0.34668)/ /0.0010
IPCM					
Heme-O ₂	11.53	1.798(1.791)/ /0.007	0.02011(0.02165) /0.0015	-0.3270(-0.3243) /0.0027	0.35034 (0.34689)/ /0.0035
Heme-CO	7.121	1.755(1.753)/ /0.002	0.02011 (0.02067)/ /0.0005	-0.2756(-0.2751) /0.0005	0.35034 (0.34982)/ /0.0005
Heme-NO	9.013	1.776(1.769)/ /0.005	0.02011 (0.02080)/ /0.0007	-0.3094(-0.3080) /0.0014	0.35034 (0.34953)/ /0.0008
SCIPCM					
Heme-O ₂	12.02	1.801(1.793)/	0.01998(0.02191)	-0.3278(-0.3255)	0.34986(0.33457)/

		/0.008	/0.0020	/0.0023	/0.0033
Heme-CO	7.466	1.761(1.758)/ /0.003	0.01998 (0.02294)/ /0.0003	-0.2759(-0.2756) /0.0003	0.34986 (0.34916)/ /0.0007
Heme-NO	9.521	1.780(1.776)/ /0.004	0.01998 (0.02059)/ /0.0006	-0.3099(-0.3083) /0.0016	0.34986 (0.34881)/ /0.0010

Table 4. The occupation number labeled as ON with corresponding energies presented and the selected charge transfer energies of the Heme models in carbon tetrachloride phase (kcal mol⁻¹)

NBO parameters	E ² _{LP-σ*N-H}	ON _{(LP)/ Δn_{LP}}	ON _{σ*NH/Δn_{σ*NH}}	E _{LP/ ΔE_{LP}}	E _{σ*NH/ ΔE_{σ*NH}}
1CCl4					
Heme-O ₂	14.89	1.921(1.902) 0.019	0.01663 (0.03261)/ 0.016	-0.3795(-0.3746) /0.0049	0.39355 (0.35558)/ 0.038
Heme-CO	7.023	1.898(1.893) 0.005	0.01663 (0.02059)/ 0.004	-0.3573(-0.3557) /0.0016	0.39355 (0.38052)/ 0.013
Heme-NO	8.986	1.912(1.899) 0.013	0.01663 (0.02887) /0.012	-0.3691(-0.3659) /0.0032	0.39355 (0.36758)/ 0.026
2 CCl4					
Heme-O ₂	14.15	1.921(1.905) 0.016	0.01663 (0.03116) /0.015	-0.3684(-0.607) /0.0041	0.39355 (0.35756)/ 0.036
Heme-CO	6.856	1.899(1.895) 0.004	0.01663 (0.02018)/ 0.004	-0.3502 (-0.3487) /0.0015	0.39355 (0.38457)/ 0.009
Heme-NO	8.074	1.911(1.899) 0.012	0.01663 (0.02555)/ 0.009	-0.3567(-0.3543) /0.0024	0.39355 (0.37552)/ 0.018
PCM/CCl4					
Heme-O ₂	14.10	1.922(1.904) 0.018	0.01873(0.03215) /0.014	-0.3593(-0.3555) /0.0038	0.35972(0.32476)/ 0.035
Heme-CO	6.731	1.898(1.896) 0.002	0.01873 (0.02037)/ 0.002	-0.3498(-0.3481) /0.0017	0.35972 (0.35274)/ 0.007
Heme-NO	8.156	1.910(1.898) 0.012	0.01873 (0.02983)/ 0.011	-0.3544(-0.3518) /0.0026	0.35972 (0.33877)/ 0.021
IPCM/CCl4					
Heme-	14.11	1.926(1.909)	0.01748(0.03293)	-0.3634(-0.3594)	0.36236(0.32534)/

O2		0.017	/0.015	/0.004	0.037
Heme-CO	6.724	1.899(1.895) 0.004	0.01748 (0.01909)/ 0.002	-0.3521(-0.3502) /0.0019	0.36236 (0.35338)/ 0.009
Heme-NO	8.197	1.910(1.897) 0.013	0.01748 (0.02856)/ 0.011	-0.3612(-0.3583) /0.0029	0.36236 (0.33831)/ 0.024
SCIPCM /CCl4					
Heme-O2	14.22	1.927(1.911) 0.016	0.01801(0.03265) /0.014	-0.3611(-0.3569) /0.0042	0.35683(0.32187)/ 0.035
Heme-CO	6.431	1.901(1.898) 0.003	0.01801 (0.02059)/ 0.002	-0.3486(-0.3473) /0.0013	0.35683 (0.34786)/ 0.009
Heme-NO	8.576	1.912(1.899) 0.013	0.01801 (0.02804)/ 0.010	-0.3568(-0.3540) /0.0028	0.35683 (0.33881)/ 0.018

Table 5. The calculated stretching vibrational frequencies (cm^{-1}) of investigated Heme models, stretching vibrational frequencies difference (in cm^{-1}) and Espinosa HB energies (kcal mol^{-1}) at the B3LYP/6-311G(d,p) level in solvents and gas phase

parameters	E(HB)Spinosa	V(N-H) _{Hist}	V(N-H) _{My}	$\Delta v(\text{N} - \text{H})$
Gas phase				
Heme-O2	39.5	3506.7463	3420.9873	85.759
Heme-CO	36.8	3506.7463	3444.9844	61.762
Heme-NO	39.1	3506.7463	3427.1421	79.604
1H2O(CCl4)				
Heme-O2	36.2(37.9)	3506.7463	3431.7641(3421.7645)	74.982(84.982)
Heme-CO	32.1(35.6)	3506.7463	3471.6558(3459.7627)	35.090(46.984)
Heme-NO	34.5(36.6)	3506.7463	3442.9837(3423.8703)	63.763(82.876)
2H2O(CCl4)				
Heme-O2	33.6(36.6)	3506.7463	3452.8796(3422.9848)	53.867(83.762)
Heme-CO	28.1(29.5)	3506.7463	3486.9856(3460.6254)	19.761(46.121)
Heme-NO	32.0(34.3)	3506.7463	3474.7133(3425.1801)	32.033(81.566)
PCM				
Heme-O2	33.5(37.0)	3419.3422(3485.8712)	3386.7862(3422.3927)	32.556(63.479)
Heme-CO	28.5(30.1)	3419.3422(3485.8712)	3397.1163(3454.3279)	22.226(31.544)
Heme-NO	30.8(35.0)	3419.3422(3485.8712)	3391.8904(3425.9970)	27.452(59.874)
IPCM				
Heme-O2	33.9(36.9)	3426.9519(3491.9036)	3392.4478(3431.3621)	34.504(60.541)
Heme-CO	28.6(30.6)	3426.9519(3491.9036)	3405.1189(3461.1378)	21.833(30.766)
Heme-NO	30.8(34.8)	3426.9519(3491.9036)	3395.6979(3434.0802)	31.254(57.823)
SCIPCM				
Heme-O2	33.7(37.4)	3427.9877(3490.8791)	3392.0157(3429.6487)	35.972(61.231)
Heme-CO	28.7(29.7)	3427.9877(3490.8791)	3404.5327(3459.8555)	23.455(31.024)
Heme-NO	30.3(34.3)	3427.9877(3490.8791)	3394.2367(3431.8914)	33.751(58.988)

Values in parentheses refer to calculation in carbon tetra chloride solution.